

## Multiscale Dictionary Learning for MRI

S. Ravishankar<sup>1</sup>, and Y. Bresler<sup>1</sup>

<sup>1</sup>Department of Electrical and Computer Engineering and the Coordinated Science Laboratory, University of Illinois, Urbana, IL, United States

**Introduction:** The sparsity of MR images in certain transform domains has enabled Compressed Sensing (CS) [1] to obtain accurate image reconstructions from undersampled k-space data. CS methods in the past have focused on analytical sparsifying transforms such as wavelets, and finite differences or Total Variation (TV) [2] to reconstruct images. However, CS with nonadaptive sparsifying transforms is usually limited in typical MR images to 2.5-3 fold undersampling. Recent work has shown that learning adaptive transforms (*dictionaries*) can lead to superior image reconstructions [3]. The sparsity in this framework is enforced on overlapping image patches and the dictionary is directly adapted to the current image leading to higher undersampling rates. In this work, we explore the use of multiscale dictionaries for CS MRI. Such dictionaries enforce sparsity at multiple scales (image patch sizes) combining the results at those scales for superior reconstructions.

**Theory and Algorithm:** The Problem formulation (P0) for CSMRI based on multiscale dictionary learning enforces sparsity of the patches of the reconstructed image ( $x$ ) at multiple scales, and also produces a reconstruction that is consistent with the available k-space data ( $y$ ). Here,  $F_u$  is the undersampled Fourier transform;  $s$  denotes the scale (N different scales are assumed);  $R_{ij}^s$  is an operator that extracts a square image patch of size  $\sqrt{n_s} \times \sqrt{n_s}$  from  $x$ ;  $(i, j)$  indexes the top left corner of the patch in  $x$ ;  $\alpha_{ij}^s$  is the sparse representation of that patch in the scale-dictionary  $D^s$  of size  $n_s \times K_s$ , with the number of non-zeros not more than  $T_0^s$ ;  $D^s \alpha_{ij}^s$  is the sparse approximation of the patch;  $\Gamma$  is the set  $\{\alpha_{ij}^s\}_{ij,s}$ ;  $D$  is the multiscale dictionary  $\{D^s\}_s$ ; and  $v = \lambda/\sigma$  ( $\sigma$ : measurement noise level (estimate),  $\lambda$ : a positive constant).

(P0)  $\min_{x,D,\Gamma} \sum_{s=1}^N \sum_{ij} \gamma^s \|R_{ij}^s x - D^s \alpha_{ij}^s\|_2^2 + v \|F_u x - y\|_2^2$  s.t.  $\|\alpha_{ij}^s\|_0 \leq T_0^s \forall i, j, s$ . The first term in the cost of (P0) measures the quality of the sparse approximations of the image patches at different scales with respect to the scale dictionaries, with  $\gamma^s$  denoting the weighting at scale  $s$ . The second term in the cost enforces data fidelity in k-space. (P0) is solved using an alternating minimization scheme. In one step (dictionary learning),  $x$  is assumed fixed, and the multiscale dictionary  $D$  is jointly learnt with the sparse representations of the image patches at various scales,  $\Gamma$ . In the other step (reconstruction update),  $D$  and  $\Gamma$  are fixed, and  $x$  is updated to satisfy data consistency. The dictionary learning step uses the K-SVD algorithm [4] where the  $D^s$  at each  $s$  is learnt separately from the patches at that scale. The reconstruction update step involves a least squares problem that can be solved using the corresponding normal equation and employing the conjugate gradient method. A simpler solution however, updates  $x$  in k-space using the dictionary predicted values for the non-sampled Fourier frequencies and a weighted average between the dictionary predicted value and the measured value at sampled k-space locations. The dictionary prediction is

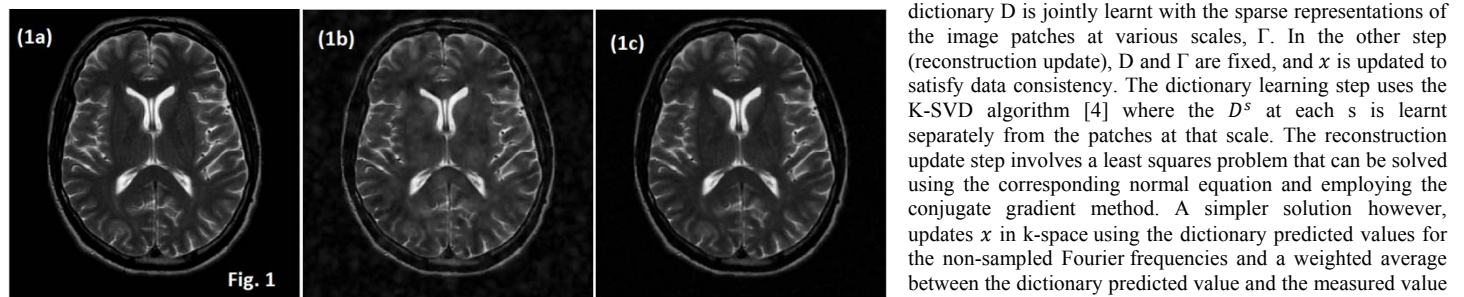


Fig. 1

obtained by taking the Fourier transform of the sparse approximation image that is obtained by averaging (weighted by  $\gamma^s$ ) the sparse approximations of image patches from various scales at their respective locations in the image. The alternating reconstruction scheme is initialized with a zero-filled Fourier reconstruction for  $x$ .

**Experiments:** We use the parameters  $N = 3$ ,  $\gamma^s = 1 \forall s$ ,  $n_1 = 9, n_2 = 16, n_3 = 25, K_s = n_s, T_0^s = 0.15 \times n_s, \lambda = 140$  for the algorithm and compare it with a leading CSMRI method [2]. Peak Signal to Noise Ratio (PSNR) in dB is indicated for the reconstructions. Fig. 1 demonstrates the performance of our algorithm on the reference image of the brain in (1a) using simulated (by subsampling the DFT) variable density 2D random sampling at 10 fold undersampling of k-space. The

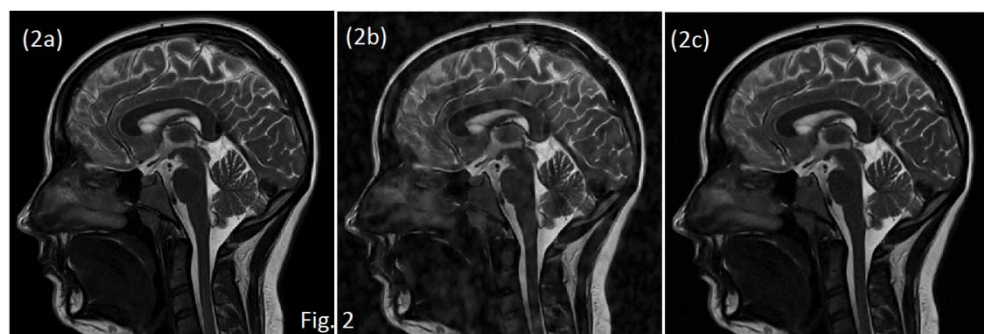


Fig. 2

cartesian FSE sequence. Randomly undersampled phase encodes of the 2D FSE were obtained in order to test the performance of the proposed reconstruction algorithm. When 5.9 fold undersampling was employed, the reconstruction of [2] with wavelets and TV shown in (1b) is seen to have many visible aliasing artifacts (26.7 dB). On the other hand, our reconstruction shown in (1c) is free of such obscuring artifacts (35.9 dB) at this high undersampling factor. Fig. 2 uses the ref. image of (2a) and performs simulated variable density random sampling of k-space at 10 fold undersampling. The reconstruction of [2] with TV shown in (2b) has large aliasing errors and a poor PSNR (26 dB). On the other hand, our formulation (P0) produces an artifact-free reconstruction in (2c) (36.6 dB). In Fig. 3, T2-weighted k-space data of a brain was acquired (by [2]) using a

reconstruction of [2] with wavelets and TV shown in (1b) is seen to have many visible aliasing artifacts (26.7 dB). On the other hand, our reconstruction shown in (1c) is free of such obscuring artifacts (35.9 dB) at this high undersampling factor. Fig. 2 uses the ref. image of (2a) and performs simulated variable density random sampling of k-space at 10 fold undersampling. The reconstruction of [2] with TV shown in (2b) has large aliasing errors and a poor PSNR (26 dB). On the other hand, our formulation (P0) produces an artifact-free reconstruction in (2c) (36.6 dB). In Fig. 3, T2-weighted k-space data of a brain was acquired (by [2]) using a

cartesian FSE sequence. Randomly undersampled phase encodes of the 2D FSE were obtained in order to test the performance of the proposed reconstruction algorithm. When 5.9 fold undersampling was employed, the reconstruction of [2] with wavelets and TV shown in (1b) is seen to have many visible aliasing artifacts (26.7 dB). On the other hand, our reconstruction shown in (1c) is free of such obscuring artifacts (35.9 dB) at this high undersampling factor.

**Discussion:** The multiscale reconstruction scheme outlined in this work is shown to give rise to substantially better reconstructions both visually and in terms of PSNR, as compared to a leading CSMRI method [2]. Reconstructions of [2] at high undersampling factors contain numerous artifacts that severely affect image quality. On the other hand, our adaptive patch-based approach exploiting scale diversity provides artifact free reconstructions even at high undersampling factors. Future work will explore the design of optimal sampling schemes for our framework as well as look at other interesting properties of the dictionary that can provide even better reconstructions for highly undersampled CSMRI. The clinical significance of the visual and quantitative improvements will need to be evaluated e.g., by expert observer task-oriented ROC studies.

**Acknowledgement:** Research supported in part by NSF grant CCF 06-35234. Fig. (1a) available at <http://www.cottageadvancedimaging.com>. The k-space data of Fig. 3 and Matlab implementation of method [2] are available at <http://www.stanford.edu/~mlustig>.

**References:** [1] Donoho D IEEE Trans Info Th 2006 ; 52:1289-1306. [2] Lustig M et al. MRM 2007; 58:1182-95. [3] Ravishankar S et al. ISBI 2011 (submitted). [4] Aharon M et al. IEEE Trans Sig Proc 2006 ; 54: 4311-22.